

# UV Resonance Raman Measurements of Poly-L-Lysine's Conformational Energy Landscapes: Dependence on Perchlorate Concentration and Temperature

Lu Ma, Zeeshan Ahmed, Aleksandr V. Mikhonin, and Sanford A. Asher\*

Department of Chemistry, University of Pittsburgh, Pittsburgh, Pennsylvania 15260

Received: January 16, 2007; In Final Form: March 23, 2007

UV resonance Raman spectroscopy has been used to determine the conformational energy landscape of poly-L-lysine (PLL) in the presence of NaClO<sub>4</sub> as a function of temperature. At 1 °C, in the presence of 0.83 M NaClO<sub>4</sub>, PLL shows an ~86%  $\alpha$ -helix-like content, which contains  $\alpha$ -helix and  $\pi$ -bulge/helix conformations. The high  $\alpha$ -helix-like content of PLL occurs because of charge screening due to strong ion-pair formation between ClO<sub>4</sub><sup>−</sup> and the lysine side chain −NH<sub>3</sub><sup>+</sup>. As the temperature increases from 1 to 60 °C, the  $\alpha$ -helix and  $\pi$ -bulge/helix conformations melt into extended conformations (PPII and 2.5<sub>1</sub>-helix). We calculate the  $\Psi$  Ramachandran angle distribution of the PLL peptide bonds from the UV Raman spectra which allows us to calculate the PLL (un)folding energy landscapes along the  $\Psi$  reaction coordinate. We observe a basin in the  $\Psi$  angle conformational space associated with  $\alpha$ -helix and  $\pi$ -bulge/helix conformations and another basin for the extended PPII and 2.5<sub>1</sub>-helical conformations.

## Introduction

The most important outstanding problem in enzymology involves the elucidation of the mechanism whereby proteins fold into their native states.<sup>1–9</sup> It is still impossible to accurately predict protein conformations from their primary sequences, unless these sequences were previously observed. Recently, the first steps in protein folding have been examined in a series of kinetic studies of small peptides in  $\beta$ -hairpins<sup>10–13</sup> and in  $\alpha$ -helices.<sup>14–23</sup> Theoretical simulations of (un)folding processes have also elucidated mechanisms of peptide folding dynamics.<sup>24–27</sup> Most recently, sophisticated vibrational spectroscopic kinetic measurements have been used to probe the earliest steps in the secondary structure (un)folding process.<sup>15,28–30</sup>

Poly-L-lysine (PLL) is a useful model system for studying protein conformational changes because it can adopt multiple conformations.<sup>31–43</sup> Its secondary structure has been characterized by numerous spectroscopic methods such as CD,<sup>44</sup> IR,<sup>35</sup> NMR,<sup>45–47</sup> vibrational Raman optical activity,<sup>48–50</sup> VCD,<sup>51</sup> and most recently by UV resonance Raman spectroscopy.<sup>36,38,52</sup> At neutral and low pH values, the lysine side chains are positively charged, and electrostatic repulsions between the side chains make PLL adopt extended conformations. For example, Mikhonin et al. recently examined the low pH conformations of PLL by using UV resonance Raman spectroscopy (UVRS),<sup>53</sup> and they demonstrated that the unfolded PLL peptides exist in an equilibrium between PPII and extended 2.5<sub>1</sub>-helix conformations. The PPII conformation is stabilized by peptide–water hydrogen bonds,<sup>54–56</sup> whereas the 2.5<sub>1</sub>-helix conformation is forced by electrostatic repulsions between neighboring lysine side chains.<sup>53</sup> These electrostatic repulsions can be decreased by adding salt,<sup>32,35,57</sup> or by raising the pH which neutralizes the side chain charges.<sup>31,35,36,38,52,58</sup> The decreased repulsions alter the PLL conformational equilibrium and allow the formation of additional conformations.

Previous studies show that ClO<sub>4</sub><sup>−</sup> is especially effective in lowering electrostatic repulsions and stabilizing the PLL helical

content at low pH.<sup>32,35,57</sup> The ClO<sub>4</sub><sup>−</sup>-induced  $\alpha$ -helix stabilization has been shown to be much larger than other singly charged anions such as Cl<sup>−</sup>.<sup>35</sup> This stabilization is consistent with the mechanism Goto et al.<sup>59</sup> proposed that ClO<sub>4</sub><sup>−</sup> forms strong ion-pairs to the lysine−NH<sub>3</sub><sup>+</sup> groups.<sup>60,61</sup>

In this work, we use UVRS to examine the temperature and NaClO<sub>4</sub> concentration dependence of the conformations of PLL. We determine the PLL (un)folding energy landscape along the  $\Psi$  reaction coordinate by utilizing the methodology developed by Mikhonin et al.<sup>62</sup> This energy landscape defines the stability and distribution of PLL between PPII, 2.5<sub>1</sub>-helix, and  $\alpha$ -helix-like conformations.

## Experimental Section

**Materials.** Poly-L-lysine HCl was purchased from Sigma (MW<sub>vis</sub> = 25 200, DP<sub>vis</sub> = 153, MW<sub>MALLS</sub> = 44 000, DP<sub>MALLS</sub> = 267. Here DP<sub>vis</sub> and DP<sub>MALLS</sub> refer to the degree of polymerization measured by viscosity and multi-angle laser light scattering, respectively), and used without further purification. Small aliquots of HCl and sodium hydroxide were used to adjust the solution pH. NaClO<sub>4</sub> was purchased from Sigma Chemical Co.

**UV Resonance Raman Instrument.** The UV resonance Raman (UVRR) instrumentation has previously been described in detail.<sup>63,64</sup> A Coherent Infinity Nd:YAG laser (Coherent, infinity) produced 355-nm, 3-ns pulses at 100 Hz. This beam was Raman-shifted to 204 nm (fifth anti-Stokes) by using a 1-m tube filled with hydrogen gas (60 psi). The sample was circulated in a free surface, temperature-controlled stream. The Raman scattered light was imaged into a subtractive double spectrometer, and the UV light was detected by a CCD camera (Princeton Instruments Co.). The UVRR spectra were measured at 1.2 mg/mL peptide concentrations.

**CD Measurements.** Circular dichroism (CD) spectra were measured by using a Jasco J-710 spectropolarimeter. The spectra were measured by using a temperature-controlled 0.2-mm path length cell at 0.64 mg/mL PLL concentrations.

\* Corresponding author. Tel: (412)-624-8570. Fax: (412)-624-0588. E-mail: asher@pitt.edu.

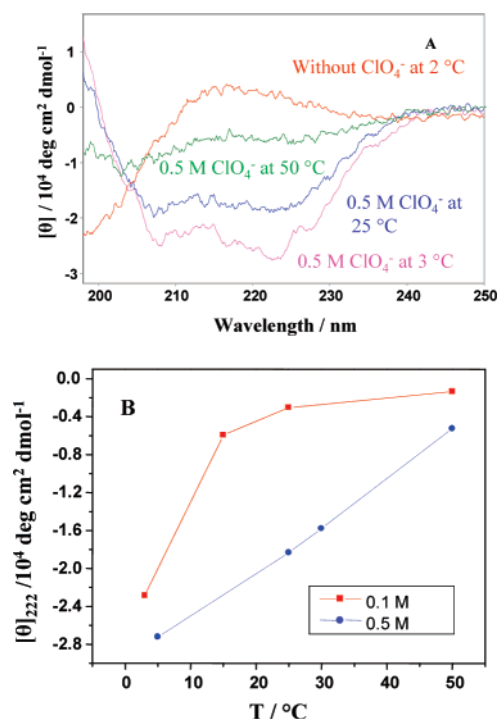


**Figure 1.** (A) CD spectra of PLL (0.64 mg/mL) at pH 6.1 containing 0.5 M NaClO<sub>4</sub> at 3 °C (pink), 25 °C (blue), 50 °C (green); in the absence of NaClO<sub>4</sub> at pH 5.5 at 2 °C (red). (B) Temperature dependence of the molar ellipticities of PLL at 222 nm containing 0.1 M (red), and 0.5 M (blue) NaClO<sub>4</sub>.

## Results and Discussion

**CD Spectra of PLL in the Absence and Presence of NaClO<sub>4</sub>.** The CD spectrum of PLL (Figure 1A) in the absence of NaClO<sub>4</sub> shows a positive band at ~218 nm and a strong negative band centered below 200 nm, which are hallmarks of PPII-like conformations in water.<sup>65,66</sup> However, in the presence of 0.1 and 0.5 M NaClO<sub>4</sub> concentrations, the CD spectra show significant  $\alpha$ -helical-like content, as indicated by the negative band at 222 nm. The increasing in the 222-nm molar ellipticity indicates that the  $\alpha$ -helix-like conformations melt as the temperature increases from 1 to 50 °C (Figure 1A). The difference in the two melting curves shown in Figure 1B clearly demonstrates that NaClO<sub>4</sub> stabilizes  $\alpha$ -helix-like structures. In 0.1 M NaClO<sub>4</sub>, the  $\alpha$ -helix-like conformations are almost fully melted by 20 °C, whereas in presence of 0.5 M NaClO<sub>4</sub>, they persist until 50 °C. This increased stability of  $\alpha$ -helix-like conformations appears to derive from the electrostatic screening of charges on the peptide chains by specific ion-pairing of ClO<sub>4</sub><sup>-</sup> anions with the lysine-NH<sub>3</sub><sup>+</sup> groups.<sup>59,61,67</sup>

**204-nm UV Raman Spectra of Unfolded PLL.** We examined the unfolded state of PLL at pH 5.5 by measuring the 204-nm UV resonance Raman spectra in the absence of NaClO<sub>4</sub>. At these conditions, lysine side chains are fully ionized, so the electrostatic repulsion prevents the formation of  $\alpha$ -helix-like conformations. As shown in Figure 2, at pH 5.5, the PLL spectra show an AmI band at 1665 cm<sup>-1</sup> (predominantly a C=O stretching vibration), while the AmII band is located at 1560 cm<sup>-1</sup> (C-N stretching coupled with N-H b). The resonance enhancement of the C $\alpha$ -H b band at ~1395 cm<sup>-1</sup> results from the coupling between C $\alpha$ -H b and N-H b motions.<sup>58,68</sup> This coupling is largest for extended  $\beta$ -strand/PPII conformations, and it is negligible for  $\alpha$ -helix-like conformations. Hence, the C $\alpha$ -H b band intensity is indicative of conformations other than  $\alpha$ -helix, 3<sub>10</sub>-helix, and  $\pi$ -helix.<sup>38,68</sup>

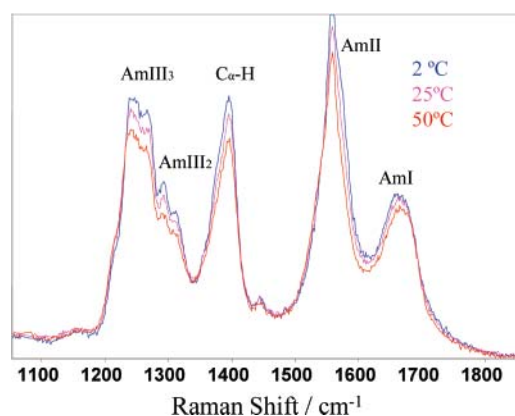


**Figure 2.** UVRR spectra (204-nm) of PLL in the absence of NaClO<sub>4</sub> at pH 5.5 at 2, 25, and 50 °C.

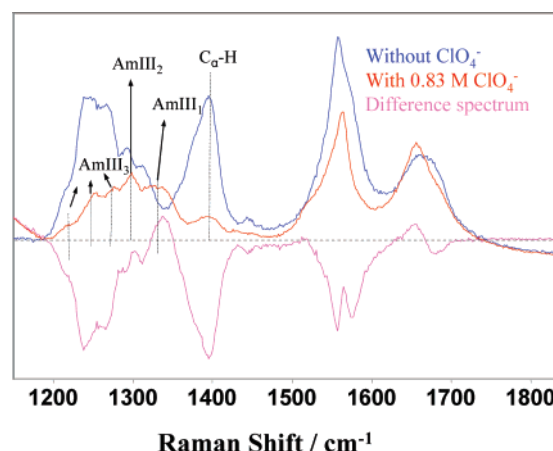


**Figure 3.** Raman spectra (204-nm) of PLL in the presence and absence of NaClO<sub>4</sub> and their difference spectrum at 1 °C. The AmII band doublet in the difference spectrum results from over-subtraction of the O<sub>2</sub> Raman band.

The conformation-sensitive AmIII region between ~1200 and 1350 cm<sup>-1</sup> mainly involves N-H bending and C-N stretching motions. This region is complicated, and we recently reassigned it in detail.<sup>69–71</sup> The PLL AmIII<sub>2</sub> region shows a doublet at 1312 and 1293 cm<sup>-1</sup>, while the AmIII<sub>3</sub> region shows peaks at ~1270 and 1243 cm<sup>-1</sup>, and a shoulder at 1212 cm<sup>-1</sup>. Our pH 5.5 PLL spectra are similar to Mikhonin et al.'s PLL spectra at pH 2.<sup>53</sup> Hence, we conclude that the 1270 cm<sup>-1</sup> band derives from a 2.5<sub>1</sub>-helix conformation, while the 1243 cm<sup>-1</sup> band derives from the PPII conformation.

**Spectral Changes Associated with NaClO<sub>4</sub>-Induced Folding of PLL.** The Figure 3 Raman spectra show that, at 1 °C, addition of 0.83 M NaClO<sub>4</sub> induces the formation of  $\alpha$ -helix-like conformations.<sup>58</sup> The PLL spectrum in the presence of NaClO<sub>4</sub> shows an AmI band at 1657 cm<sup>-1</sup> and an AmII band at 1563 cm<sup>-1</sup>. A much weaker C $\alpha$ -H b band occurs at ~1395 cm<sup>-1</sup>, while the AmIII<sub>1</sub> and AmIII<sub>2</sub> bands are located at ~1332 and 1297 cm<sup>-1</sup>, respectively. The conformation-sensitive AmIII<sub>3</sub> band is decreased in intensity and shows a shoulder at 1218 cm<sup>-1</sup> and peaks at 1253 and 1276 cm<sup>-1</sup> with greatly decreased intensities. The difference spectrum (Figure 3) shows troughs at the C $\alpha$ -H b band position and in the AmIII region which derive from the loss of the PPII and 2.5<sub>1</sub>-helix conformations.<sup>58,63,71</sup>

**The Assignment of the AmIII Region Bands of PLL in the Folded State.** We can calculate the pure  $\alpha$ -helical PLL spectrum by subtracting the appropriate amount of PPII and 2.5<sub>1</sub>-helical PLL from the measured spectrum containing

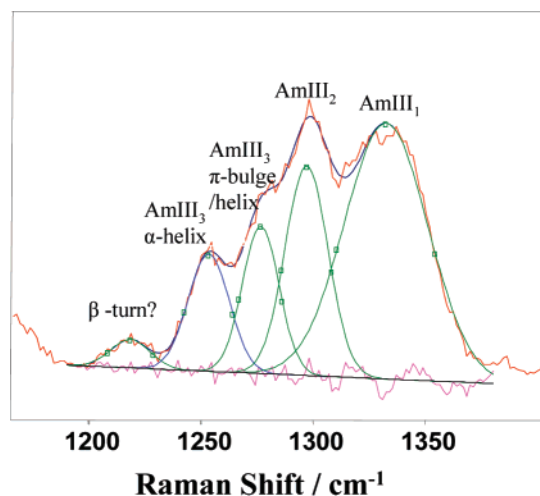


**Figure 4.** Deconvolution of the AmIII region of the calculated helical PLL spectrum into a sum of 5 Gaussian bands. The helix spectrum is calculated by subtracting the appropriate amounts of the spectra with the extended PLL conformation from the measured spectrum.

**TABLE 1: Spectral AmIII Band Assignment of PLL Peptide**

band	frequency (cm <sup>-1</sup> )
AmIII <sub>1</sub>	1332
AmIII <sub>2</sub>	1296
AmIII <sub>3</sub> (π-bulge/helix)	1276
AmIII <sub>3</sub> (α-helix)	1253
AmIII <sub>3</sub> <sup>†</sup> (β-turn)	1218

NaClO<sub>4</sub>.<sup>63,71</sup> The AmIII region of this calculated α-helical-like PLL spectrum can be well-modeled by five Gaussian bands (Figure 4). The AmIII<sub>1</sub> and AmIII<sub>2</sub> bands are located at ~1332 and ~1300 cm<sup>-1</sup>, respectively. The AmIII<sub>3</sub> region shows three peaks at 1276, 1253, and 1218 cm<sup>-1</sup> indicating the presence of multiple conformations in equilibrium.

According to the method developed by Mikhonin et al.,<sup>62</sup> which calculates the Ψ angle distribution from the AmIII<sub>3</sub> band frequency distributions, given the known hydrogen bonding state of the peptide bonds,<sup>14,62,68</sup> the 1276 and 1253 cm<sup>-1</sup> AmIII<sub>3</sub> bands derive from conformations with average Ramachandran Ψ angles of -62° and -36°, respectively. The Ψ angle values most likely derive from π-bulge/helix conformation (Ψ = -70° for an ideal π-helix) and an α-helix conformation (Ψ = -47°). It has been found that the Ψ dihedral value of π-bulges, a common deformation of α-helices, shows a distribution of values.<sup>72</sup> Mikhonin et al.<sup>73</sup> found Ψ values of π-bulges/helices for the ala-based AP peptide of -58°, very close to our result. Our Ψ dihedral values also are consistent with numerous recent reports of the π-bulges/helices in model peptides.<sup>22,72,74–77</sup>

The 1218 cm<sup>-1</sup> band, which also appears in the spectra of extended PLL (Figure 2), probably derives from β-turn conformations.<sup>62</sup> It could derive from either type I, I', II, or II' β-turns et al.<sup>62</sup> These AmIII band assignments are listed in Table 1.

**Thermal Melting of α-Helix and π-Bulge/Helix Conformations.** We examined the temperature dependence of PLL's NaClO<sub>4</sub>-induced α-helix-like conformations by measuring the 204-nm UV resonance Raman spectra between 1 and 60 °C (Figure 5). As the temperature increases, we observe a continuous increase in the C<sub>α</sub>-H b band intensity and AmIII<sub>3</sub> band intensities of the 1270, 1240, and 1220 cm<sup>-1</sup> bands, indicating melting of the α-helix and π-bulge/helix conformations. The high-temperature PLL spectra are similar to PLL spectra in the absence of NaClO<sub>4</sub> (Figure 5A). The thermally unfolded

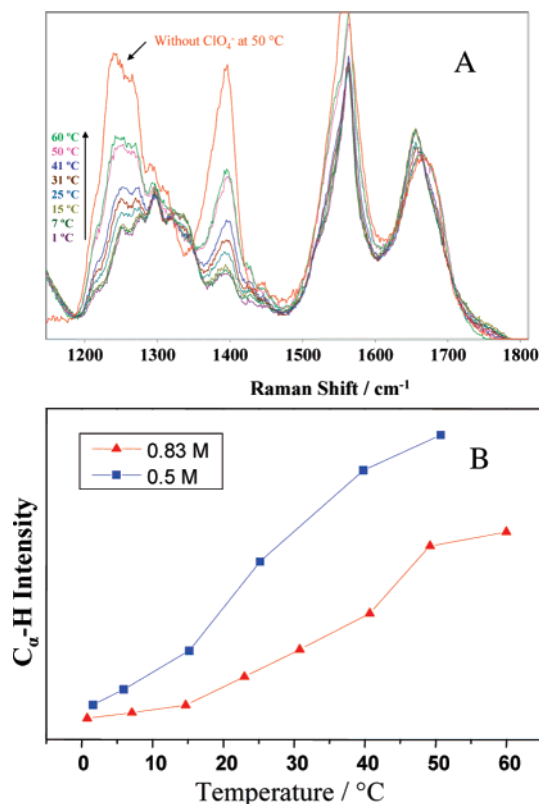


**Figure 5.** (A) Temperature dependence of the UVRR spectra of PLL containing 0.83 M NaClO<sub>4</sub> at pH 5.2. The red spectrum is the PLL Raman spectrum without NaClO<sub>4</sub> at 50 °C. The temperature-induced melting of PLL in the presence of 0.5 M NaClO<sub>4</sub> is similar to that in 0.83 M NaClO<sub>4</sub>. (B) Temperature dependence of C<sub>α</sub>-H b band Raman intensity. The spectra were normalized using the ClO<sub>4</sub><sup>-</sup> band intensity.

conformational equilibrium of PLL in the presence of NaClO<sub>4</sub> is similar to the conformational equilibrium for the charged side chains at low ionic strength which are dominated by PPII and 2.5<sub>1</sub>-helix conformations.<sup>53</sup> The Raman spectra in Figure 5A show multiple isosbestic points which suggest that the melting of the α-helix-like conformations is a “two-state” transition from a mixture of α-helix and π-bulge/helix conformations to a mixture of PPII and 2.5<sub>1</sub>-helix conformations.

Figure 5B shows the temperature dependence of the C<sub>α</sub>-H b band Raman intensity which is a non-α-helical conformational marker.<sup>38,68</sup> The melting curve for the 0.5 M NaClO<sub>4</sub> PLL solution shows a *T<sub>m</sub>* ~ 35 °C, while the 0.83 M NaClO<sub>4</sub> solution *T<sub>m</sub>* is increased to ~65 °C. These Raman results agree with the CD results discussed above.

We can estimate the change in the number of α-helical-like amide bonds from the observed increased intensity of the C<sub>α</sub>-H b band. For PLL samples containing ClO<sub>4</sub><sup>-</sup>, we normalized the amide band intensities with respect to the known Raman cross sections of ClO<sub>4</sub><sup>-</sup>. Using Dudik et al.'s data<sup>78</sup> for the absolute Raman cross section of the 932 cm<sup>-1</sup> band of ClO<sub>4</sub><sup>-</sup> at 204-nm excitation, we calculated the Raman cross sections for the amide bands of PLL in the presence of ClO<sub>4</sub><sup>-</sup>:

$$\sigma_A = (I_{Am} N_{ClO_4} \sigma_{ClO_4}) / (n_A N_P I_{ClO_4}) \quad (1)$$

where  $\sigma_A$  and  $\sigma_{ClO_4}$  are the Raman cross sections of an amide band and the 932 cm<sup>-1</sup> ClO<sub>4</sub><sup>-</sup> band, respectively.  $N_{ClO_4}$  and  $N_P$  are the number of ClO<sub>4</sub><sup>-</sup> and PLL molecules in the scattering volume, respectively.  $I_{ClO_4}$  and  $I_{Am}$  are the integrated intensity of the ClO<sub>4</sub><sup>-</sup> (932 cm<sup>-1</sup>) and the amide bands, respectively.  $n_A$



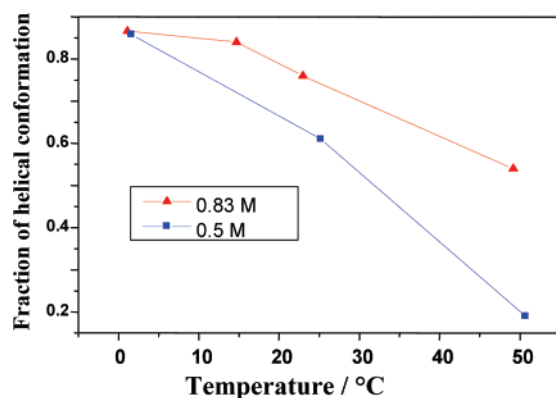


**Figure 6.** Temperature dependence of the fraction of  $\alpha$ -helix-like conformations in the presence of 0.83 and 0.5 M  $\text{ClO}_4^-$  at pH 5.2.

**TABLE 2: Calculated Cross Section of PLL Peptide in Extended Conformations**

band	cross section (mbarn molecule <sup>-1</sup> sr <sup>-1</sup> )
$\text{C}_\alpha\text{--H}$ bending	60
AmI	75

is the number of amide peptide bonds in PLL contributing to the intensity of the amide band.

In cases where  $\text{ClO}_4^-$  is not present, the amide band intensities of the unfolded state were normalized to the AmI band intensity, which we earlier showed was the least sensitive to secondary structural changes.<sup>58,63,68,71</sup> Using the AmI band cross section, we can calculate the  $\text{C}_\alpha\text{--H}$  b band cross sections in the absence of  $\text{NaClO}_4$ . The calculated cross sections of PLL amide bands in the extended conformations are listed in Table 2.

From the  $\text{C}_\alpha\text{--H}$  b band cross sections we can calculate the number of non- $\alpha$ -helical amide bonds in PLL as

$$n_A = (I_{\text{C}_\alpha\text{H}} N_{\text{ClO}_4} \sigma_{\text{ClO}_4}) / (\sigma_{\text{C}_\alpha\text{H}} N_P I_{\text{ClO}_4}) \quad (2)$$

We calculate that at 1 °C, in the presence of 0.83 M  $\text{NaClO}_4$ , PLL has an 86%  $\alpha$ -helix-like content.

We can calculate the number of  $\alpha$ -helix and  $\pi$ -bulge/helix peptide bonds which melt as

$$\delta n_A = (-\delta I_{\text{C}_\alpha\text{H}} N_{\text{ClO}_4} \sigma_{\text{ClO}_4}) / (\sigma_{\text{C}_\alpha\text{H}} N_P I_{\text{ClO}_4}) \quad (3)$$

where  $\delta n_A$  is number of  $\alpha$ -helix and  $\pi$ -bulge bonds lost or gained and  $\delta I_{\text{C}_\alpha\text{H}}$  is the change in the normalized integrated  $\text{C}_\alpha\text{--H}$  bending band intensity. In 0.83 M  $\text{NaClO}_4$ , the integrated intensity of the  $\text{C}_\alpha\text{--H}$  b band at 50 °C is 32% larger than that at 1 °C. The helix melting curves are displayed in Figure 6.

Our results agree with Jiji et al.'s<sup>52</sup> data that at pH 11.6 at 10 °C, PLL shows a ~85%  $\alpha$ -helical content. At pH 11.6, the lysine side chains are neutralized, which eliminates the electrostatic repulsions which destabilize the  $\alpha$ -helices at lower pH. The fact that at pH 5.2 addition of 0.83 M  $\text{NaClO}_4$  results in ~86%  $\alpha$ -helical-like content suggests that the charged side chains are neutralized by  $\text{NaClO}_4$ .<sup>59–61,79</sup>

**$\Psi$  Population Distributions.** The AmIII<sub>3</sub> bands are significantly broadened compared to the AmIII<sub>3</sub> band of peptide crystals.<sup>14</sup> The band breadth is largely due to an inhomogeneous distribution of  $\Psi$  angles. We calculated the inhomogeneous frequency distributions of the observed AmIII<sub>3</sub> bands and the  $\Psi$  dihedral angle distributions of the PLL peptide bonds (Figure 7) by using the methodology developed by Mikhonin et al.<sup>14,53,62</sup>

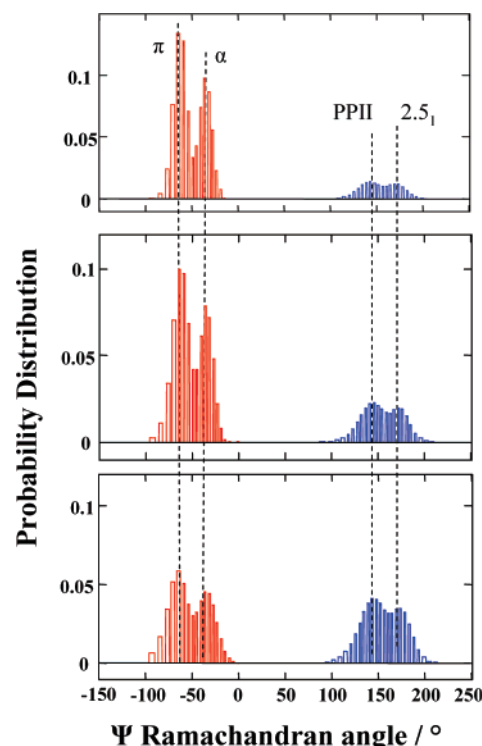


**Figure 7.** Temperature dependence of  $\Psi$  angle distribution of PLL containing 0.83 M  $\text{NaClO}_4$  at 1, 25, and 50 °C.

(We assume equal Raman cross sections for two  $\alpha$ -helix-like conformations, PPII and 2.5<sub>1</sub>-helix conformations.)

In the helical region (red), we calculate high concentrations of  $\pi$ -helical ( $\Psi = -80$  to  $-50^\circ$ ) and  $\alpha$ -helical ( $\Psi = -50$  to  $-15^\circ$ ) conformations. Similarly, in the extended, non-helical region (blue) we observe significant populations of PPII ( $\Psi = 110$  to  $160^\circ$ ) and 2.5<sub>1</sub>-helix ( $\Psi = 150$  to  $200^\circ$ ) conformations.

As discussed above, the 1218  $\text{cm}^{-1}$  AmIII<sub>3</sub> band likely derives from a  $\beta$ -turn conformation.  $\beta$ -turns, which result from water-inserted hydration of  $\alpha$ -helices, was proposed by Sundaralingam et al. to be intermediates in the helix-coil transition pathway.<sup>80</sup> Unfortunately, a lack of suitable models limits our ability to quantitate the contributions of  $\beta$ -turn at 1218  $\text{cm}^{-1}$ .

As the temperature increases from 1 to 50 °C, the concentrations of the  $\alpha$ -helix-like conformations decrease, while the PPII and 2.5<sub>1</sub>-helix conformations increase. However, the relative population ratios of the PPII to 2.5<sub>1</sub>-helix, and the  $\alpha$ -helix to  $\pi$ -bulge/helix conformations show little change. This suggests that these pairs of conformationally similar structures are separated by small energy differences. This result further confirms that PLL unfolds by a “two-state” mechanism where it goes from compact  $\alpha$ -helix and  $\pi$ -bulge/helix conformations to extended PPII and 2.5<sub>1</sub>-helices.

**Conformational Free Energy Landscapes for PLL (Un)folding.** The probability that the PLL peptide bond is found at a particular  $\Psi_i$  angle state depends on the Gibbs free energy ( $G_i$ ) of this  $\Psi_i$  dihedral angle. Assuming equal degeneracies of the different conformations, the energy difference between a conformation at  $\Psi_i$  angle and another conformation at  $\Psi_0$  angle is

$$\Delta G_{i-0} = -N_A k_B T \ln \frac{n(\psi_i)}{n(\psi_0)} \quad (4)$$

where  $N_A$  is the Avogadro number,  $k_B$  is the Boltzmann constant,

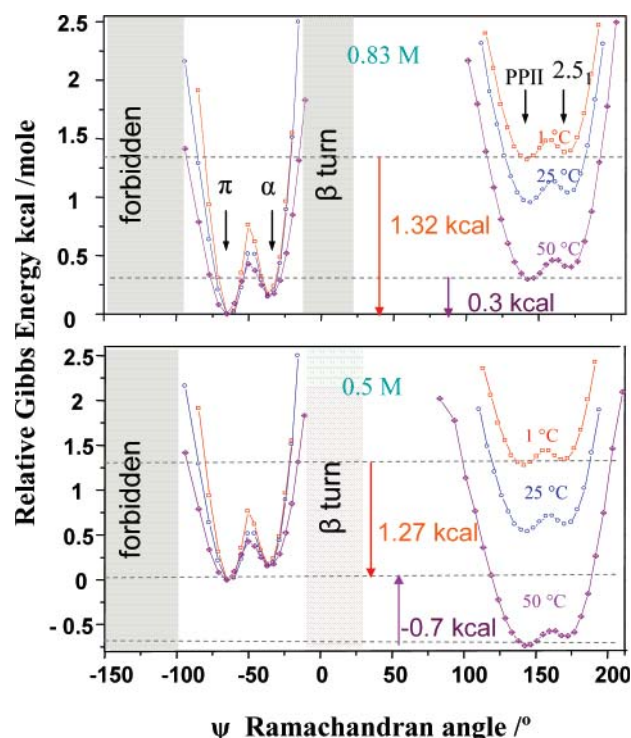


**Figure 8.** Estimated Gibbs free energy landscape for PLL (1.2 mg/mL) at 0.83 and 0.5 M NaClO<sub>4</sub> concentration at 1 (red), 25 (blue), and 50 °C (purple).

$T$  is the temperature, and  $n(\psi_i)/n(\psi_0)$  is the ratio of populations with Ramachandran angles  $\Psi_i$  and  $\Psi_0$ .

Using eq 4, we calculate the Gibbs free energies of the populated equilibrium conformations relative to that of the  $\pi$ -bulge conformation (Figure 8). We find an energy landscape with two basins. One is associated with the  $\alpha$ -helix and  $\pi$ -bulge/helix conformations, while the other is associated with the PPII and 2.5<sub>1</sub>-helix conformations.

At 1 °C, in the presence of 0.83 M NaClO<sub>4</sub>, the  $\alpha$ -helix conformational energy lies above that of the  $\pi$ -bulge/helix by only  $\sim 170$  cal/mol, and the energy barrier between the  $\alpha$ -helix and the  $\pi$ -bulge/helix is  $\sim 760$  cal/mol higher than the  $\pi$ -bulge minimum. This barrier decreases somewhat as the temperature increases.

Similarly, at 1 °C the 2.5<sub>1</sub>-helix conformational energy lies  $\sim 64$  cal/mol above that of the PPII conformation. Previously, Mikhonin et al. found at pH 2 a similar energy difference of  $\sim 74$  cal/mol between the PPII and 2.5<sub>1</sub>-helix conformations.<sup>53</sup>

At 1 °C, the  $\pi$ -bulge is stabilized over the PPII conformation by  $\sim 1.32$  and  $\sim 1.27$  kcal/mol energy in the presence of 0.83 M NaClO<sub>4</sub> and 0.5 M NaClO<sub>4</sub>, respectively. As the temperature increases from 1 to 50 °C, the PLL PPII and 2.5<sub>1</sub>-helix conformational energy decrease relative to that of the  $\pi$ -bulge. For 0.83 M NaClO<sub>4</sub>, we observe that the PPII/2.5<sub>1</sub>-helix conformational energy is greater than that of the  $\alpha$ -helix-like conformation until the temperature increases to 50 °C. In contrast, the energy of the extended PPII conformation at 50 °C in 0.5 M NaClO<sub>4</sub> is  $\sim 0.7$  kcal/mol below that of the  $\alpha$ -helix conformation.

**Thermodynamic Parameters for PLL “Two-State” Transition.** Assuming that the enthalpy difference is independent of temperature, we can estimate the enthalpy and entropy changes for the  $\alpha$ -helix-like conformations melting which are  $\Delta H = 12 \pm 1.6$  kcal/mol,  $\Delta S = 39 \pm 5$  cal/mol·K in the presence of 0.5 M NaClO<sub>4</sub>, and  $\Delta H = 6.1 \pm 0.8$  kcal/mol,  $\Delta S = 19 \pm 3$  cal/mol·K in the presence of 0.83 M NaClO<sub>4</sub>.

The change in the slope of the melting curve as the NaClO<sub>4</sub> concentration increases from 0.5 to 0.83 M allows us to calculate that the magnitude of both  $\Delta H$  and  $\Delta S$  for melting decreases  $\sim 2$ -fold. We observe an apparent loss of cooperativity in the thermal unfolding transition at high NaClO<sub>4</sub> concentrations.

We expect that much of this change derives from the water solvent. Surprisingly, little change is observed in water activity between these NaClO<sub>4</sub> concentrations.<sup>81</sup> Thus, the change in the thermodynamic parameters must derive from energetic perturbations in the conformations of the two states. To have additional insight, we need additional structural insights to determine the origin of these changes.

## Conclusions

The presence of NaClO<sub>4</sub> induces a conformational change in PLL from extended PPII/2.5<sub>1</sub>-helix conformations to folded  $\alpha$ -helix and  $\pi$ -bulge/helix conformations. As the temperature increases, the compact helical conformations melt to extended conformations. Increasing the NaClO<sub>4</sub> concentrations shifts the  $T_m$  of the unfolding transition to higher values indicating an increased stability of the helical conformations at higher NaClO<sub>4</sub> concentration. The Raman isosbestic points suggest that the PLL melting is a “two-state” transition from a mixture of compact helical conformations to extended PPII and 2.5<sub>1</sub>-helix conformations. We were able to roughly estimate the enthalpy and entropy change of the melting transition. We also calculated the energy landscape along the  $\Psi$  folding coordinate. The neutralization of the lysine  $-\text{NH}_3^+$  groups by efficient ion pairing with  $\text{ClO}_4^-$  dramatically impacts the energy landscape which changes the equilibrium peptide conformations.

**Acknowledgment.** We gratefully acknowledge Dr. Natalya Myshakina, Dr. Jon Scaffidi, Konstantin Pimenov, Bhavya Sharma, and Sergei Bykov for useful discussions. We thank Dr. Ken Jordan, Dr. Steve Weber, and Dr. Chris Schafmeister for useful suggestions. This work was supported by NIH Grant GM8RO1EB002053-24.

## References and Notes

- (1) Creighton, T. E. *Protein Folding*; W. H. Freeman: New York, 1992.
- (2) Baldwin, R. L.; Rose, G. D. *Trends Biochem. Sci.* **1999**, *24*, 26.
- (3) Baldwin, R. L.; Rose, G. D. *Trends Biochem. Sci.* **1999**, *24*, 77.
- (4) Dill, K. A. *Protein Sci.* **1999**, *8*, 1166.
- (5) Dobson, C. M.; Sali, A.; Karplus, M. *Angew. Chem., Int. Ed.* **1998**, *37*, 868.
- (6) Oliveberg, M.; Tan, Y.-J.; Silow, M.; Fersht, A. R. *J. Mol. Biol.* **1998**, *277*, 933.
- (7) Wright, P. E.; Dyson, H. J. *J. Mol. Biol.* **1999**, *293*, 321.
- (8) Myers, J. K.; Oas, T. G. *Annu. Rev. Biochem.* **2002**, *71*, 783.
- (9) Alm, E.; Baker, D. *Proc. Natl. Acad. Sci. U.S.A.* **1999**, *96*, 11305.
- (10) Blanco, F. J.; Jimenez, M. A.; Herranz, J.; Rico, M.; Santoro, J.; Nieto, J. L. *J. Am. Chem. Soc.* **1993**, *115*, 5887.
- (11) Colley, C. S.; Griffiths-Jones, S. R.; George, M. W.; Searle, M. S. *Chem. Commun.* **2000**, 593.
- (12) Dinner, A. R.; Lazaridis, T.; Karplus, M. *Proc. Natl. Acad. Sci. U.S.A.* **1999**, *96*, 9068.
- (13) Fesinmeyer, R. M.; Hudson, F. M.; Andersen, N. H. *J. Am. Chem. Soc.* **2004**, *126*, 7238.
- (14) Asher, S. A.; Mikhonin, A. V.; Bykov, S. B. *J. Am. Chem. Soc.* **2004**, *126*, 8433.
- (15) Huang, C.-Y.; Klemke, J. W.; Getahun, Z.; DeGrado, W. F.; Gai, F. *J. Am. Chem. Soc.* **2001**, *123*, 9235.
- (16) Lednev, I. K.; Karnoup, A. S.; Sparrow, M. C.; Asher, S. A. *J. Am. Chem. Soc.* **2001**, *123*, 2388.
- (17) Ramajo, A. P.; Petty, S. A.; Starzyk, A.; Decatur, S. M.; Volk, M. *J. Am. Chem. Soc.* **2005**, *127*, 13784.
- (18) Mikhonin, A. V.; Asher, S. A. *J. Phys. Chem. B* **2005**, *109*, 3047.
- (19) Thompson, P. A.; Munoz, V.; Jas, G. S.; Henry, E. R.; Eaton, W. A.; Hofrichter, J. *J. Phys. Chem. B* **2004**, *104*, 378.
- (20) Fesinmeyer, R. M.; Peterson, E. S.; Dyer, R. B.; Andersen, N. H. *Protein Sci.* **2005**, *14*, 2324.

- (21) Luo, P.; Baldwin, R. L. *Proc. Natl. Acad. Sci. U.S.A.* **1999**, *96*, 4930.
- (22) Shirley, W. A.; Brooks, C. L., III. *Proteins* **1997**, *28*, 59.
- (23) Millhauser, G. I.; Stenland, C. J.; Hanson, P.; Bolin, K. A.; van de Ven, F. J. M. *J. Mol. Biol.* **1997**, *267*, 963.
- (24) Shakhnovich, E. I. *Curr. Opin. Struct. Biol.* **1997**, *7*, 29.
- (25) Karplus, M.; Sali, A. *Curr. Opin. Struct. Biol.* **1995**, *5*, 58.
- (26) Dill, K. A.; Chan, H. S. *Nat. Struct. Biol.* **1997**, *4*, 10.
- (27) Bryngelson, J. D.; Onuchic, J. N.; Socci, N. D.; Wolynes, P. G. *Proteins* **1995**, *21*, 167.
- (28) Munoz, V.; Thompson, P. A.; Hofrichter, J.; Eaton, W. A. *Nature* **1997**, *390*, 196.
- (29) Williams, S.; Causgrove, T. P.; Gilmanshin, R.; Fang, K. S.; Callender, R. H.; Woodruff, W. H.; Dyer, R. B. *Biochemistry* **1996**, *35*, 691.
- (30) Lednev, I. K.; Karnoup, A. S.; Sparrow, M. C.; Asher, S. A. *J. Am. Chem. Soc.* **1999**, *121*, 4076.
- (31) Davidson, B.; Fasman, G. D. *Biochemistry* **1967**, *6*, 1616.
- (32) Dearborn, D. G.; Wetlaufer, D. B. *Biochem. Biophys. Res. Commun.* **1970**, *39*, 314.
- (33) Drake, A. F.; Siligardi, G.; Gibbons, W. A. *Biophys. Chem.* **1988**, *31*, 143.
- (34) Makarov, A. A.; Adzhubel, I. A.; Protasevich, I. I.; Lobachov, V. M.; Fasman, G. D. *Biopolymers* **1994**, *34*, 1123.
- (35) Painter, P. C.; Koenig, J. L. *Biopolymers* **1976**, *15*, 229.
- (36) Song, S.; Asher, S. A. *J. Am. Chem. Soc.* **1989**, *111*, 4295.
- (37) Tiffany, M. L.; Krimm, S. *Biopolymers* **1969**, *8*, 347.
- (38) Wang, Y.; Purrello, R.; Jordan, T.; Spiro, T. C. *J. Am. Chem. Soc.* **1991**, *113*, 6359.
- (39) Yaron, A.; Katchalski, E.; Berger, A.; Fasman, G. D.; Sober, H. A. *Biopolymers* **1971**, *10*, 1107.
- (40) Yu, N. T. *Crit. Rev. Biochem.* **1977**, *4*, 229.
- (41) Yu, T. J.; Lippert, J. L.; Peticolas, W. L. *Biopolymers* **1973**, *12*, 2161.
- (42) Vorobjev, Y. N.; Scheraga, H. A. *J. Phys. Chem.* **1995**, *99*, 7180.
- (43) Ashton, L.; Barron, L. D.; Czarnik-Matusewicz, B.; Hecht, L.; Hyde, J.; Blanch, E. W. *Mol. Phys.* **2006**, *104*, 1429.
- (44) Tiffany, M. L.; Krimm, S. *Biopolymers* **1968**, *6*, 1379.
- (45) Darke, A.; Finer, E. G. *Biopolymers* **1975**, *14*, 441.
- (46) Joubert, F. J.; Lotan, N.; Scheraga, H. A. *Physiol. Chem. Phys. Med. NMR* **1969**, *1*, 348.
- (47) Perly, B.; Chevalier, Y.; Chachaty, C. *Macromolecules* **1981**, *14*, 969.
- (48) McColl, I. H.; Blanch, E. W.; Gill, A. C.; Rhie, A. G. O.; Ritchie, M. A.; Hecht, L.; Nielsen, K.; Barron, L. D. *J. Am. Chem. Soc.* **2003**, *125*, 10019.
- (49) Barron, L. D.; Hecht, L.; Blanch, E. W.; Bell, A. F. *Prog. Biophys. Mol. Biol.* **2000**, *73*, 1.
- (50) Wilson, G.; Hecht, L.; Barron, L. D. *J. Chem. Soc., Faraday Trans.* **1996**, *92*, 1503.
- (51) Keiderling, T. A.; Silva, R. A.; Yoder, G.; Dukor, R. K. *Bioorg. Med. Chem.* **1999**, *7*, 133.
- (52) JiJi, R. D.; Balakrishnan, G.; Hu, Y.; Spiro, T. G. *Biochemistry* **2006**, *45*, 34.
- (53) Mikhonin, A. V.; Myshakina, N. S.; Bykov, S. V.; Asher, S. A. *J. Am. Chem. Soc.* **2005**, *127*, 7712.
- (54) Shi, Z.; Chen, K.; Liu, Z.; Kallenbach, N. R. *Chem. Rev.* **2006**, *106*, 1877.
- (55) Eker, F.; Griebenow, K.; Schweitzer-Stenner, R. *J. Am. Chem. Soc.* **2003**, *125*, 8178.
- (56) Poon, C. D.; Samulski, E. T. *J. Am. Chem. Soc.* **2000**, *122*, 5642.
- (57) Bello, J. *Biopolymers* **1992**, *32*, 185.
- (58) Chi, Z.; Chen, X. G.; Holtz, J. S. W.; Asher, S. A. *Biochemistry* **1998**, *37*, 2854.
- (59) Goto, Y.; Takahashi, N.; Fink, A. L. *Biochemistry* **1990**, *29*, 3480.
- (60) Ebert, G.; Kuroyanagi, Y. *Polymer* **1982**, *23*, 1147.
- (61) Ebert, G.; Kuroyanagi, Y. *Polymer* **1982**, *23*, 1154.
- (62) Mikhonin, A. V.; Bykov, S. V.; Myshakina, N. S.; Asher, S. A. *J. Phys. Chem. B* **2006**, *110*, 1928.
- (63) Lednev, I. K.; Karnoup, A. S.; Sparrow, M. C.; Asher, S. A. *J. Am. Chem. Soc.* **1999**, *121*, 8074.
- (64) Bykov, S. V.; Lednev, I. K.; Ianoul, A.; Mikhonin, A. V.; Asher, S. A. *Appl. Spectrosc.* **2005**, *59*, 1541.
- (65) Tiffany, M. L.; Krimm, S. *Biopolymers* **1972**, *11*, 2309.
- (66) Woody, R. W. *Adv. Biophys. Chem.* **1992**, *2*, 37.
- (67) Shibue, M.; Mant, C. T.; Hodges, R. S. *J. Chromatogr., A* **2005**, *1080*, 49.
- (68) Asher, S. A.; Ianoul, A.; Mix, G.; Boyden, M. N.; Karnoup, A.; Diem, M.; Schweitzer-Stenner, R. *J. Am. Chem. Soc.* **2001**, *123*, 11775.
- (69) Lee, S.; Krimme, S. *Biopolymers* **1998**, *46*, 283.
- (70) Diem, M.; Lee, O.; Roberts, G. M. *J. Phys. Chem.* **1992**, *96*, 548.
- (71) Mikhonin, A. V.; Ahmed, Z.; Ianoul, A.; Asher, S. A. *J. Phys. Chem. B* **2004**, *108*, 19020.
- (72) Cartailier, J.-P.; Luecke, H. *Structure* **2004**, *12*, 133.
- (73) Mikhonin, A. V.; Asher, S. A. *J. Am. Chem. Soc.* **2006**, *128*, 13789.
- (74) Sudha, R.; Kohtani, M.; Breaux, G. A.; Jarrold, M. F. *J. Am. Chem. Soc.* **2004**, *126*, 2777.
- (75) Armen, R.; Alonso, D. O. V.; Daggett, V. *Protein Sci.* **2003**, *12*, 1145.
- (76) Mahadevan, J.; Lee, K.-H.; Kuczera, K. *J. Phys. Chem. B* **2001**, *105*, 1683.
- (77) Fodje, M. N.; Al-Karadaghi, S. *Protein Eng.* **2002**, *15*, 353.
- (78) Dudik, J. M.; Johnson, C. R.; Asher, S. A. *J. Chem. Phys.* **1985**, *82*, 1732.
- (79) Hoshino, M.; Goto, Y. *J. Biochem.* **1994**, *116*, 910.
- (80) Sundaralingam, M.; Sekharudu, Y. C. *Science* **1989**, *244*, 1333.
- (81) Dutkiewicz, E.; Jakubowska, A. *ChemPhysChem* **2002**, *3*, 221.